AIP Advances

Charge transport studies in donor-acceptor block copolymer PDPP-TNT and PC71BM based inverted organic photovoltaic devices processed in room conditions

Cite as: AIP Advances 5, 077177 (2015); https://doi.org/10.1063/1.4927763
Submitted: 17 April 2015 . Accepted: 15 July 2015 . Published Online: 31 July 2015

Shashi B. Srivastava, Prashant Sonar, and Samarendra P. Singh

COLLECTIONS

Paper published as part of the special topic on Chemical Physics, Energy, Fluids and Plasmas, Materials Science and Mathematical Physics

openaccess

View Online Export Citation CrossMark

ARTICLES YOU MAY BE INTERESTED IN

Effect of leakage current and shunt resistance on the light intensity dependence of organic solar cells
Applied Physics Letters 106, 083301 (2015); https://doi.org/10.1063/1.4913589

Polymer solar cells: P3HT:PCBM and beyond
Journal of Renewable and Sustainable Energy 10, 013508 (2018); https://doi.org/10.1063/1.5012992

Two-layer organic photovoltaic cell
Applied Physics Letters 48, 183 (1986); https://doi.org/10.1063/1.96937

Call For Papers!
AIP Advances
SPECIAL TOPIC: Advances in Low Dimensional and 2D Materials

AIP Publishing

© 2015 Author(s).

Charge transport studies in donor-acceptor block copolymer PDPP-TNT and PC71BM based inverted organic photovoltaic devices processed in room conditions

Shashi B. Srivastava,[1] Prashant Sonar,[2] and Samarendra P. Singh[1,a]
[1]*Department of Physics, Shiv Nadar University, Gautam Buddha Nagar, Uttar Pradesh, India-201307*
[2]*School of Chemistry, Physics and Mechanical Engineering, Queensland University of Technology, Brisbane, Australia-4001*

(Received 17 April 2015; accepted 15 July 2015; published online 31 July 2015)

Diketopyrrolopyrole-naphthalene polymer (PDPP-TNT), a donor-acceptor co-polymer, has shown versatile behavior demonstrating high performances in organic field-effect transistors (OFETs) and organic photovoltaic (OPV) devices. In this paper we report investigation of charge carrier dynamics in PDPP-TNT, and [6,6]-phenyl C_{71} butyric acid methyl ester (PC71BM) bulk-heterojunction based inverted OPV devices using current density-voltage (J-V) characteristics, space charge limited current (SCLC) measurements, capacitance-voltage (C-V) characteristics, and impedance spectroscopy (IS). OPV devices in inverted architecture, ITO/ZnO/PDPP-TNT:PC71BM/MoO_3/Ag, are processed and characterized at room conditions. The power conversion efficiency (PCE) of these devices are measured ~3.8%, with reasonably good fill-factor 54.6%. The analysis of impedance spectra exhibits electron's mobility $\sim 2 \times 10^{-3}$ $cm^2V^{-1}s^{-1}$, and lifetime in the range of 0.03-0.23 ms. SCLC measurements give hole mobility of 1.12×10^{-5} $cm^2V^{-1}s^{-1}$, and electron mobility of 8.7×10^{-4} $cm^2V^{-1}s^{-1}$. *© 2015 Author(s). All article content, except where otherwise noted, is licensed under a Creative Commons Attribution 3.0 Unported License.* [http://dx.doi.org/10.1063/1.4927763]

I. INTRODUCTION

Bulk heterojunction based organic photovoltaic (OPV) devices have witnessed significant improvement in their performance up to ~10% over last few years.[1,2] In order to harness potential applications of OPV devices towards realizing low-cost, low-temperature processable and flexible solar cells, intense efforts are being made.[3] These efforts are focused around developing high performing air-stable organic small molecules and polymers, and optimizing device performances by introducing different functional interfacial layers of organic or inorganic materials in conventional or inverted device structures.[4,5] Inverting the device architecture makes OPVs less prone to ambient degradation and offers better air-stability by opening more choices of materials.[6,7] Further, an in-depth investigation of dynamics and recombination kinetics of charge carriers is essential to know underlying physics of OPV devices.[5,8] A combination of characterization tools are needed to apply in order to establish the dependence of electrical parameters of OPV devices on the properties of individual organic materials, the morphology of bulk heterojunction active layers, and the energetics at various interfaces involved in devices. We believe such studies will pave the way to understand existing device performance limiting factors, and to develop OPV devices into a mature technology.

Designing of conjugated molecular structures having electron donor (D) and electron acceptor (A) moieties in polymer backbone has been an effective approach to develop high performing donor

[a]Author to whom correspondence should be addressed. Electronic mail: samarendra.singh@snu.edu.in.

 ©Author(s) 2015

for realizing efficient OPV devices. Poly{3,6-dithiophene-2-yl-2,5-di(2-octyldodecyl)-pyrrolo [3,4-c] pyrrole-1,4-dione-alt-naphthalene} (PDPP-TNT) is one of such polymer having naphthalene and diketopyrrolopyrrole (DPP) as donor and acceptor moieties in the polymer backbone, respectively. PDPP-TNT has shown good performance in organic field-effect transistors (OFETs) and OPV devices processed under inert ambient (in a dry N_2 filled glove box).[9,10] In OFETs, PDPP-TNT has exhibited hole mobility (μ_h) of 0.65 $cm^2V^{-1}s^{-1}$ and 0.98 $cm^2V^{-1}s^{-1}$ measured in single and dual gate OFET device geometries, respectively.[9] The conventional OPV devices based on a blend active layer of PDPP-TNT (donor) and PC71BM (acceptor) has shown power conversion efficiency (PCE) of 4.7 %.[9] Such promising behavior of PDPP-TNT organic semiconducting polymer in both OFET and OPV devices makes it an interesting material to study the charge transport properties and recombination kinetics.

In this paper, we report an investigation of charge dynamics in PDPP-TNT:PC71BM bulk heterojunction based inverted OPV devices processed and characterized under room conditions. These inverted OPV devices exhibit PCE ~3.8 %. The performance of these OPV devices is stable over more than a month which enable us to execute a series of experiments in room ambient. We have performed space-charge limited current (SCLC) measurements, capacitance-voltage (C-V) measurements and impedance spectroscopy (IS) to study charge carrier transport, their accumulation, and recombination kinetics in PDPP-TNT:PC71BM bulk heterojunction active layer, and their OPV devices.

II. EXPERIMENTAL DETAILS

Inverted OPV devices were fabricated on patterned indium tin oxide (ITO) substrates with a configuration of ITO/ZnO/PDPP-TNT:PC71BM/MoO_3/Ag. The molecular structure of PDPP-TNT and PC71BM, and a schematic of inverted OPV device are shown in Fig. 1. ITO coated glass substrates were cleaned using soap solution (2% micro-90) in de-ionized (DI) water for 20 minutes. The substrates were then rinsed with DI water, and sonicated in acetone and isopropanol, respectively. Next, the substrates were dried with N_2 gun, and treated with UV-ozone for 20 minutes. A sol-gel of ZnO (0.45 M) was prepared using zinc acetate in 2-methoxyethanol and ethanolamine.[11] The prepared solution was spin coated at 2000 rpm for 60 seconds to deposit ZnO thin film (~40 nm) on the substrate. A drying process was performed on a hot plate at 250 °C for 15 minutes in room ambient.[11] The PDPP-TNT was synthesized as described earlier, and PC71BM was used as it was received from Lumtec, Taiwan.[9] The PDPP-TNT:PC71BM blend layer was deposited by spin-coating a solution (15 mg/ml) of PDPP-TNT (33 wt%) and $PC_{71}BM$ (67 wt%) in a mixture of chloroform and o-dichlorobenzene (4:1 by volume) at 5000 rpm for 60 seconds on top of ZnO layer.[9] The PDPP-TNT:PC71BM layer was annealed on a hot plate at 60 °C for 10 min

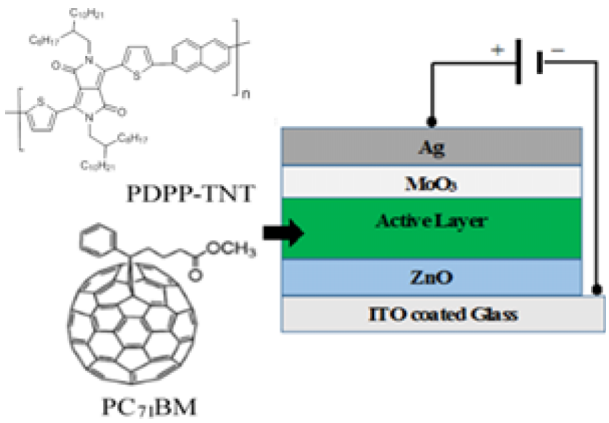

FIG. 1. Device architecture of inverted PDPP-TNT:PC71BM BHJ solar cells with chemical structures of the active layer components.

to remove the excess solvent. The thickness of the active layer used in these devices is ~150 nm. Molybdenum tri-oxide (MoO_3), an electron blocking layer, was deposited on top of the active layer by thermal evaporation. A silver cathode (100 nm) was deposited by thermal evaporation through a shadow mask under a pressure of $\sim 10^{-6}$ mbar to complete the device, resulting a device area of approximately 0.09 cm^2. For SCLC measurements, hole only devices were prepared by replacing the ZnO layer of the inverted OPV structure by thermally evaporated MoO_3 thin film resulting in the final device structure as, ITO/MoO_3/PDPP-TNT:PC71BM/MoO_3/Ag. Similarly, electron only devices were made by replacing MoO_3/Ag by Aluminum (Al), and the final device structure was ITO/ZnO/PDPP-TNT:PC71BM/Al.

Current density-voltage (J-V) characteristics of OPV devices were measured under an AM1.5G illumination source (1000 Wm^{-2}) using a Photo Emission Solar Simulator (Model #SS50AAA). The light intensity was adjusted with a NREL calibrated Si solar cell. The Keithley 4200 SCS parameter analyzer was used for the measurement of J-V characteristics of OPV devices.

The impedance analyzer (Autolab PGSTAT-302N) was used for C-V measurement, and impedance spectroscopy. Impedance spectra were recorded by applying a small voltage perturbation (10 mV) at frequencies ranging from 1 MHz to 1 Hz.

III. EXPERIMENTAL RESULTS AND DISCUSSIONS

Current-voltage (J-V) curve for ITO/ZnO/PDPP-TNT:PC71BM/MoO_3/Ag, measured in room conditions is shown in Fig. 2. The extracted parameters for optimized inverted OPV devices are: a short circuit current (J_{sc}) of 8.9 mA/cm^2, open circuit voltage (V_{oc}) of 0.79 V, fill factor (FF) of 54.6 %, and power conversion efficiency (PCE) of 3.8 %. High V_{oc} is attributed to lower highest occupied molecular orbital (HOMO) energy level of PDPP-TNT polymer. The fill factor value of the device is reasonably good and it can be attributed to lower recombination losses and low series resistance.[12]

The investigation of hole and electron mobilities in the blend active layer is extremely important in order to get the insight about the charge transport behavior in organic solar cell. Using SCLC technique, charge carrier mobilities can be determined by using electrodes that suppresses the injection of either electrons or holes, resulting in hole- or electron-only devices, respectively. J-V characteristic shows the experimental dark current densities of PDPP-TNT:PC71BM blends that were measured in hole-only and electron-only devices (Fig. 3). The SCLC region, for which the dependence of current on voltage is quadratic, has been shown with a solid blue lines for both cases. Such observation is common for low mobility disordered semiconductors, and it allows the direct

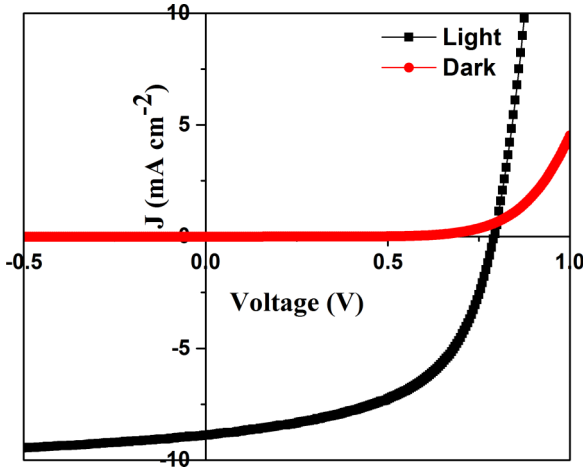

FIG. 2. Current-voltage (J-V) characteristic of inverted PDPP-TNT:PC71BM BHJ solar cells under light (black), and in dark (red) measured in room ambient.

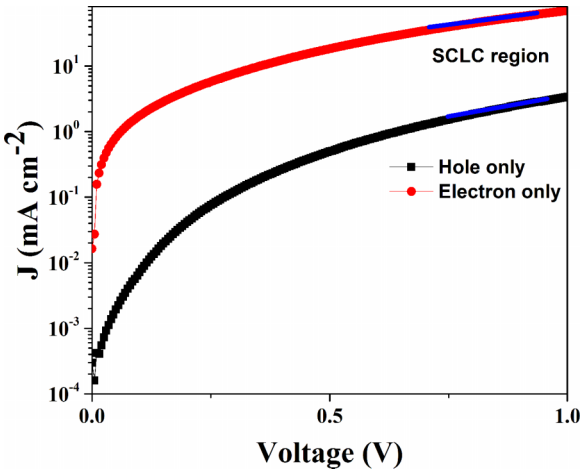

FIG. 3. Current-voltage (J-V) characteristic (in dark) for hole-only (black), and electron-only (red) devices. Blue lines shows SCLC region.

determination of charge carrier mobility.[13–15] The determined hole mobility is 1.12×10^{-5} $cm^2V^{-1}s^{-1}$ and electron mobility is 8.7×10^{-4} $cm^2V^{-1}s^{-1}$.

The capacitance-voltage (C-V) characteristic, shown in Fig. 4, illustrates a plateau in reverse and low forward voltage indicating a depletion condition. This result is imperative of formation of depletion region at BHJ/ZnO interface. Beyond a certain forward bias voltage, the capacitance starts to increase which can be explained as a result of reduction in the depletion width. The physical parameters were extracted using Mott-Schottky relation,

$$C^{-2} = \frac{2(V_{bi} - V)}{A^2 q \varepsilon \varepsilon_0 N_A} \tag{1}$$

where, V is the applied bias, V_{bi} is the built-in potential, A is the device area, q is the elementary charge, ε is the relative dielectric constant, ε_0 is the vacuum permittivity, N_A is the concentration of acceptor impurity. The Mott-Schottky analysis of C-V results, shown in Fig. 4, results built-in potential (V_{bi}) equals to 0.77 V, and the concentration of acceptor impurities (N_A) equals to $1.5 \times 10^{+16}$ /cm^3, assuming relative dielectric permittivity ε = 3 for PDPP-TNT:PC71BM blend

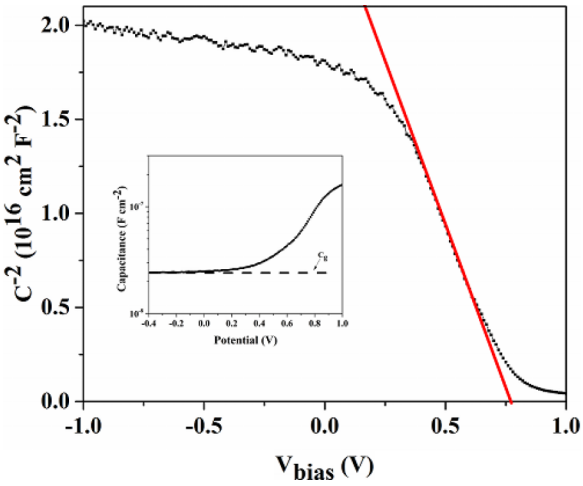

FIG. 4. Capacitance-voltage (C-V) characteristic of PDPP:TNT-PC71BM BHJ based inverted OPV devices. Characteristic capacitance (C_g) is shown in inset image.

system. The built-in voltage is related to BHJ/ZnO interface and does not set a limit to the photovoltage in the solar cell.[16] The C-V characteristics measured over reverse and low forward bias range exhibits the geometrical capacitance ~2.13 nF as compared to the calculated capacitance ~1.53 nF. It is originated by the voltage-modulation of the depletion zone built up at the cathode contact, which collapses to the geometrical capacitance near zero voltage.[17]

Fig. 5 shows the experimental Nyquist plot for different forward bias voltage (0.6-0.9 V) measured under dark condition. It can be noted that the Nyquist plot is composed of a semicircle in the lower frequency regime, and a nearly straight line for the high frequency region (inset Fig. 5). The diameter of the semicircle reduces with the increasing bias voltage which can be attributed to the reduction of impedance due to higher forward bias voltages. In order to take in account the inhomogeneous nature of interfaces in BHJ active layer in OPV devices we have used the constant phase element (CPE) based model as reported by Bisquert *et al*., and Xu *et al*.[18,19] The equivalent circuit is shown in inset Fig. 5, and it consists of a series resistance R_s, a transport resistance r_t, a capacitance C_g, and a recombination resistance r_{rec} in parallel with a CPE. These electrical circuit components signify certain physical mechanism in OPV devices. The R_s is the resistance from contact layers and electrodes, and Cg is the device capacitance associated with the depletion region formed within the active layer. In CPE based model, a parallel combination of the r_t with the geometrical capacitance, C_g, contributes to the high-frequency region of the impedance response in the Nyquist plot. Similarly, a parallel combination of the r_{rec} with CPE takes in to account the internal charge transfer events including accumulation and recombination, and contributes to the low-frequency response.[20–22] The random characteristics of active layer in OPV devices can be attributed to the distribution of relaxation times, and is related to impedance as $Z = Y_0^{-1}(j\omega)^{-n}$, where Y_0 is the coefficient of the CPE and n represents an "ideality" factor characteristic of the distribution of relaxation times.[19] n varies from 0 to 1.0, with 1.0 corresponding to pure capacitive behavior.

The equivalent circuit with appropriately chosen parameters fits the data over the entire frequency range of the measurement. It is observed that fitted value of ideality factor varies from 0.75 to 0.45 with forward bias voltage changing from 0.6 to 0.9 V, which indicates the presence of capacitive and resistive elements in the BHJ active layer. From the fitted data we notice an increase in the depression of semicircle with the increase in bias voltage. As forward bias voltage increases, conductivity of the active layer increases which reduces the accumulation of charge carriers, and hence capacitive characteristics decrease.

The chemical capacitance (C_μ), which reflects carrier accumulation in the bulk active layer, is calculated using the equation

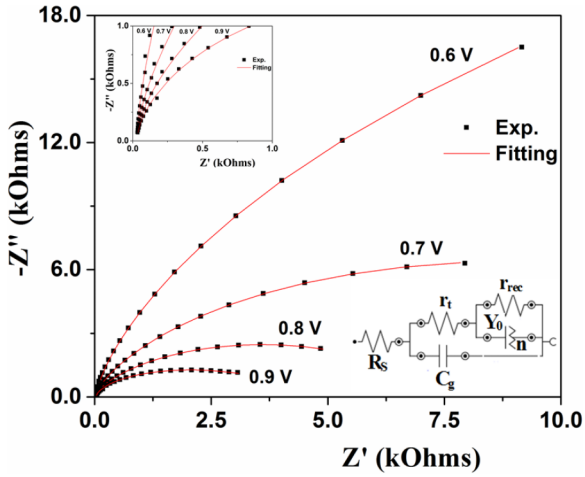

FIG. 5. Impedance response of inverted PDPP-TNT:PC71BM BHJ solar cells with different bias voltages under dark condition (Upper inset: high frequency region). The color scheme for experimental data is black and red for fitted data simulated. Equivalent circuit for the impedance spectra (Lower inset).

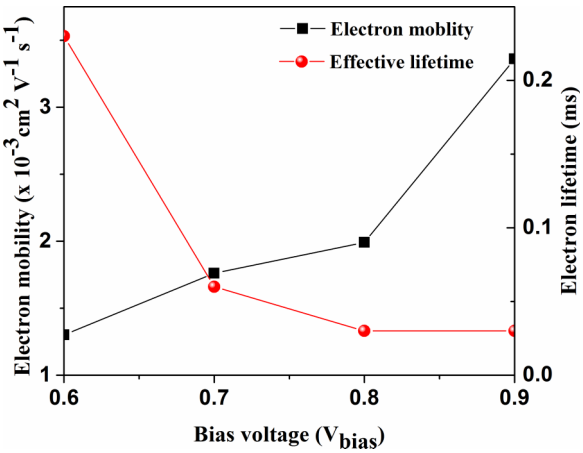

FIG. 6. Variation of electron mobility and life time determined from fitting parameters with respect to bias voltages.

TABLE I. Mobility and effective life time of electron estimated from impedance analysis.

Bias Voltage under Dark (V_{bias})	Diffusion Length (D_n) (nm)	Transit time (τ_d) (μ-sec)	Electron Mobility (μ_n) ($cm^2/V-sec$)	Effective lifetime (τ_n) (μ-sec)
0.6	3.3	7.5	1.3×10^{-3}	230
0.7	4.4	5.6	1.8×10^{-3}	60
0.8	4.5	4.9	2.0×10^{-3}	28
0.9	8.4	2.9	3.4×10^{-3}	28

$$C_\mu = \frac{(Y_0 r_{rec})^{\frac{1}{n}}}{r_{rec}}, \tag{2}$$

where Y_0 and n are the parameters of CPE, and are obtained using equivalent circuit fitting. In order to calculate characteristic time related to electron diffusion *i.e.*, transit time $\tau_d = r_t C_\mu$, and effective life time *i.e.* $\tau_n = r_{rec} C_\mu$, the chemical potential (C_μ) is calculated using equation-2.[23] Furthermore, electron diffusion length is calculated using following formula:[24]

$$D_n = \frac{L^2}{\tau_d}. \tag{3}$$

Here $L = 150$ nm is thickness of the active layer and τ_d is the diffusion time. The mobility of electrons (minority carriers) is calculated using $\mu_n = eD_n/k_BT$ (Nernst–Einstein relationship), where k_BT is the thermal energy.[25,26] The electron mobility, calculated from the fitting parameters, is found in the range of $(1.3 - 3.4) \times 10^{-3}$ $cm^2V^{-1}s^{-1}$ and it increases as the applied forward bias voltage increases, as shown in Fig. 6. The key results extracted from impedance analysis is summarized in Table I. Such field dependence of mobility is characteristic of disordered organic semiconductors.[27] This mobility value is in good agreement with the same estimated by SCLC measurements done on electron only devices. Electron's lifetime decreases with increase in applied forward bias as shown in Fig. 6. Such bias dependence of electron's life time is attributed to losses due to charge carrier recombination processes.[23]

IV. CONCLUSION

In conclusion, C-V analysis shows that the BHJ/ZnO contacts exhibit characteristic of a Schottky diode in the dark. Built-in potential is estimated to be 0.77 V with acceptor carrier concentration $\sim 10^{+16}$ /cm^3. Our study to understand the diffusion and recombination processes through impedance analysis allows us to determine diffusion length and effective life-time of charge carriers.

Electron mobility, diffusion length and effective life-time were determined using equivalent circuit model consisting of device capacitance, a CPE with various resistive elements. Electron mobility in the range of $(1.3 - 3.4) \times 10^{-3}$ $cm^2V^{-1}s^{-1}$ and effective life-time 0.03-0.25 ms for forward bias in the range of 0.6-0.9V is observed. SCLC measurement on PDPP-TNT:PC71BM BHJ active layer results electron mobility of 8.7×10^{-4} $cm^2V^{-1}s^{-1}$ and hole mobility of 1.12×10^{-5} $cm^2V^{-1}s^{-1}$. Here we notice a comparable electron mobility estimated by SCLC and impedance analysis. Hole mobility estimated by SCLC is fairly close to the same determined using time of flight (TOF) measurement done on 1.6 μm thick PDPP-TNT polymer based diode.[28] Our analysis of charge transport in PDPP-TNT:PC71BM OPV device gives us insight about field-dependent charge transport properties which enables us to further optimize various interfaces to enhance efficiency.

ACKNOWLEDGMENTS

Authors acknowledge Dr. Santosh Kumar and Dr. Priya Johari for critical reading of the manuscript and their suggestions.

[1] Martin A. Green, Keith Emery, Yoshihiro Hishikawa, Wilhelm Warta, and Ewan D. Dunlop, Progress in Photovoltaics: Research and Applications **20**(1), 12 (2012).
[2] M. C. Scharber and N. S. Sariciftci, Progress in polymer science **38**(12), 1929 (2013).
[3] Gang Li, Rui Zhu, and Yang Yang, Nature Photonics **6**(3), 153 (2012).
[4] Ivan Litzov and Christoph Brabec, Materials **6**(12), 5796 (2013).
[5] Antonio Guerrero, Núria F. Montcada, Jon Ajuria, Ikerne Etxebarria, Roberto Pacios, Germà Garcia Belmonte, and Emilio Palomares, Journal of Materials Chemistry A **1**(39), 12345 (2013).
[6] Zhicai He, Chengmei Zhong, Shijian Su, Miao Xu, Hongbin Wu, and Yong Cao, Nature Photonics **6**(9), 593 (2012).
[7] Safakath Karuthedath, Tobias Sauermann, Hans-Joachim Egelhaaf, Reinhold Wannemacher, Christoph J. Brabec, and Larry Lüer, J. Mater. Chem. A **3**(7), 3399 (2015).
[8] Tyler K. Mullenbach, Yunlong Zou, James Holst, and Russell J. Holmes, Journal of Applied Physics **116**(12), 124513 (2014).
[9] Prashant Sonar, Samarendra P Singh, Yuning Li, Zi-En Ooi, Tae-jun Ha, Ivy Wong, Mui Siang Soh, and Ananth Dodabalapur, Energy & Environmental Science **4**(6), 2288 (2011).
[10] Thelese Ru Bao Foong, Samarendra Pratap Singh, Prashant Sonar, Zi-En Ooi, Khai Leok Chan, and Ananth Dodabalapur, Journal of Materials Chemistry **22**(39), 20896 (2012).
[11] Steven K. Hau, Hin-Lap Yip, Nam Seob Baek, Jingyu Zou, Kevin O'Malley, and Alex K. Y. Jen, Applied Physics Letters **92**(25), 253301 (2008).
[12] Ikerne Etxebarria, Antonio Guerrero, Josep Albero, Germà Garcia-Belmonte, Emilio Palomares, and Roberto Pacios, Organic Electronics **15**(11), 2756 (2014).
[13] V. D Mihailetchi, L. J A Koster, P. W M Blom, C. Melzer, B. de Boer, J. K J van Duren, and R. A J Janssen, Advanced Functional Materials **15**(5), 795 (2005).
[14] C. Melzer, E. J Koop, V. D Mihailetchi, and P. W M Blom, Advanced Functional Materials **14**(9), 865 (2004).
[15] Chiatzun Goh, R. Joseph Kline, Michael D. McGehee, Ekaterina N. Kadnikova, and Jean M. J. Fréchet, Applied Physics Letters **86**(12), (2005).
[16] Juan Bisquert, David Cahen, Gary Hodes, Sven Rühle, and Arie Zaban, The Journal of Physical Chemistry B **108**(24), 8106 (2004).
[17] Francisco Fabregat-Santiago, Germa Garcia-Belmonte, Ivan Mora-Sero, and Juan Bisquert, Physical Chemistry Chemical Physics **13**(20), 9083 (2011).
[18] J. Bisquert, G. Garcia-Belmonte, P. Bueno, E. Longo, and L. O. S. Bulhões, Journal of Electroanalytical Chemistry **452**(2), 229 (1998).
[19] Liang Xu, Yun-Ju Lee, and Julia W. P. Hsu, Applied Physics Letters **105**(12), 2178 (2014).
[20] Benjamin J. Leever, Christopher A. Bailey, Tobin J. Marks, Mark C. Hersam, and Michael F. Durstock, Advanced Energy Materials **2**(1), 120 (2012).
[21] Juan Bisquert and Germà Garcia-Belmonte, The Journal of Physical Chemistry Letters **2**(15), 1950 (2011).
[22] Antonio Guerrero, Stephen Loser, Germa Garcia-Belmonte, Carson J. Bruns, Jeremy Smith, Hiroyuki Miyauchi, Samuel I. Stupp, Juan Bisquert, and Tobin J. Marks, Physical Chemistry Chemical Physics **15**(39), 16456 (2013).
[23] Germà Garcia-Belmonte, Antoni Munar, Eva M. Barea, Juan Bisquert, Irati Ugarte, and Roberto Pacios, Organic Electronics **9**(5), 847 (2008).
[24] Juan Bisquert, The Journal of Physical Chemistry B **106**(2), 325 (2001).
[25] Germà Garcia-Belmonte, Juan Bisquert, and George S. Popkirov, Applied Physics Letters **83**(11), 2178 (2003).
[26] Juan Bisquert, Physical Chemistry Chemical Physics **10**(22), 3175 (2008).
[27] D. Hertel and H. Bassler, ChemPhysChem **9**(5), 666 (2008).
[28] Samarendra P. Singh, Prashant Sonar, Chellappan Vijila, Ooi Zi En, Evan Williams, Sergey Gorelik, and Ananth Dodabalapur, XVI International Workshop on the Physics of Semiconductor Devices, Dec 19-22, 2011, IIT Kanpur, India.